AMERICAN SOCIETY FOR MICROBIOLOGY | Applied and Environmental Microbiology

Transposon Mutagenesis Identifies Genes Critical for Growth of *Pseudomonas nitroreducens* TX1 on Octylphenol Polyethoxylates

Tuan Ngoc Nguyen,[a] Chen-Wei Yeh,[b] Po-Chun Tsai,[a] Kyoung Lee,[c] Shir-Ly Huang[a,d]

Institute of Microbiology and Immunology, National Yang-Ming University, Taipei, Taiwan[a]; Department of Life Sciences, National Central University, Jhongli City, Taoyuan County, Taiwan[b]; Department of Bio Health Science, Changwon National University, Kyongnam, Republic of Korea[c]; Graduate Institute of Environmental Engineering, National Central University, Jhongli City, Taoyuan County, Taiwan[d]

ABSTRACT

***Pseudomonas nitroreducens* TX1 is of special interest because of its ability to utilize 0.05% to 20% octylphenol polyethoxylates ($OPEO_n$) as a sole source of carbon. In this study, a library containing 30,000 Tn*5*-insertion mutants of the wild-type strain TX1 was constructed and screened for $OPEO_n$ utilization, and 93 mutants were found to be unable to grow on $OPEO_n$. In total, 42 separate disrupted genes were identified, and the proteins encoded by the genes were then classified into various categories, namely, information storage and processing (14.3%), cellular processes and signaling (28.6%), metabolism (35.7%), and unknown proteins (21.4%). The individual deletion of genes encoding isocitrate lyase (*aceA*), malate synthase (*aceB*), and glycolate dehydrogenase (*glcE*) was carried out, and the requirement for *aceA* and *aceB* but not *glcE* confirmed the role of the glyoxylate cycle in $OPEO_n$ degradation. Furthermore, acetaldehyde dehydrogenase and acetyl-coenzyme A (acetyl-CoA) synthetase activity levels were 13.2- and 2.1-fold higher in TX1 cells grown on $OPEO_n$ than in TX1 cells grown on succinate, respectively. Growth of the various mutants on different carbon sources was tested, and based on these findings, a mechanism involving exoscission to liberate acetaldehyde from the end of the $OPEO_n$ chain during degradation is proposed for the breakdown of $OPEO_n$.**

IMPORTANCE

Octylphenol polyethoxylates belong to the alkylphenol polyethoxylate ($APEO_n$) nonionic surfactant family. Evidence based on the analysis of intermediate metabolites suggested that the primary biodegradation of $APEO_n$ can be achieved by two possible pathways for the stepwise removal of the C_2 ethoxylate units from the end of the chain. However, direct evidence for these hypotheses is still lacking. In this study, we described the use of transposon mutagenesis to identify genes critical to the catabolism of $OPEO_n$ by *P. nitroreducens* TX1. The exoscission of the ethoxylate chain leading to the liberation of acetaldehyde is proposed. Isocitrate lyase and malate synthase in glyoxylate cycle are required in the catabolism of ethoxylated surfactants. Our findings also provide many gene candidates that may help elucidate the mechanisms in stress responses to ethoxylated surfactants by bacteria.

Octylphenol polyethoxylates ($OPEO_n$, commercial name Triton X-100) is a nonionic surfactant that belongs to the alkylphenol polyethoxylate ($APEO_n$) family. These surfactants are used in a range of industrial and household products (1, 2). $APEO_n$ structures typically consist of hydrophilic polyethoxylate chain bound to a hydrophobic moiety, such as alkylphenol or a linear primary/secondary alcohol (3). $APEO_n$ are often discharged into wastewater treatment plants or into the environment, which leads to them ultimately being degraded into shorter ethoxylate (EO) chains. Sometimes, the chains are completely removed to form nonylphenol, octylphenol, and alkylphenol monoethoxylates to triethoxylates ($APEO_n$, $n = 1$ to ~3, respectively) (4, 5). Many studies have shown that these $APEO_n$ metabolites, which have increased hydrophobicity, are more toxic than their parent compounds (6). In fact, these metabolites are able to mimic natural hormones, thus acting as endocrine disruptors when ingested by wildlife, which in turn can affect the environment and ultimately human health (7).

The fate and degradability of $APEO_n$ in the environment have received much attention (8). The biodegradation of $APEO_n$ has been studied using both pure and mixed cultures that grow solely on $APEO_n$, and several bacterial strains have been reported as being able to degrade the EO chains of $APEO_n$ (1, 8–12). Most such isolates are proteobacteria and are often members of the genus *Pseudomonas*. Nguyen and Sigoillot (13) isolated four *Pseudomonas* strains from coastal seawater that grew on $OPEO_n$, and these generated OPEO with 4 to 5 units of EO chain as the end products. John and White (14) reported a strain of *Pseudomonas putida* that grew on nonylphenol polyethoxylate ($NPEO_n$) as the sole source of carbon, and in this case, the final accumulating metabolite was identified by gas chromatography-mass spectroscopy as $NPEO_2$. Nishio et al. (15) isolated 11 strains of $OPEO_n$-utilizing bacteria from paddy field soils. One strain, *P. putida* S-5, was shown to transform $OPEO_n$ to form $OPEO_2$ and $OPEO_3$, which were the dominant metabolites accumulating under aerobic conditions. Evidence based on analysis of intermediate metab-

Received 22 June 2016 **Accepted** 25 August 2016

Accepted manuscript posted online 2 September 2016

Citation Nguyen TN, Yeh C-W, Tsai P-C, Lee K, Huang S-L. 2016. Transposon mutagenesis identifies genes critical for growth of *Pseudomonas nitroreducens* TX1 on octylphenol polyethoxylates. Appl Environ Microbiol 82:6584–6592. doi:10.1128/AEM.01907-16.

Editor: R. E. Parales, University of California—Davis

Address correspondence to Shir-Ly Huang, sl.huang@ym.edu.tw, or Kyoung Lee, klee@changwon.ac.kr.

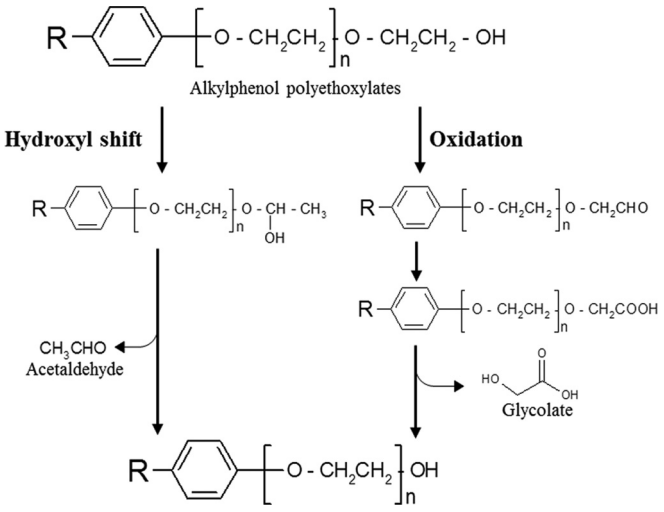

FIG 1 Proposed pathways for the biodegradation of alkylphenol polyethoxylates from the literature (14, 15, 17).

olites has suggested that the primary biodegradation of $APEO_n$ under aerobic condition is achieved by a stepwise shortening of the EO chains (13, 14, 16). Two possible pathways for the stepwise removal of the C_2 ethoxylate units from the end of the chain have been proposed (Fig. 1). The first is a nonoxidative hydroxyl shift mechanism using ether scission that yields hemiacetal, which then produces acetaldehyde (14, 17). The second is the cleavage of $APEO_n$ by terminal carboxylation, followed by hydrolysis to yield glycolate, which is oxidized to glyoxylate by glycolate dehydrogenase (15, 17). However, clear-cut evidence regarding the operation in organisms of these pathways during $OPEO_n$ degradation is still lacking.

In our previous studies, *P. nitroreducens* TX1, which possesses the ability to grow on $OPEO_n$ at a wide range of concentrations, was isolated (1, 9–12, 18). The strain is able to use 0.05% to 20% $OPEO_n$ as a sole source of carbon. The liquid chromatography-mass spectrometry (LC-MS) analysis revealed that the ethoxylate chain was sequentially shortened from the hydroxyl terminal side in this strain (9). To elucidate the biodegradation mechanism of $OPEO_n$, a library containing 30,000 mutants of strain TX1 was prepared using Tn*5* insertion mutagenesis during this study. A total of 93 mutants were identified that were unable to grow on $OPEO_n$, and these were found to have disrupted 42 individual genes. In-frame deletion of some of the target genes was then performed to confirm the roles of these genes in $OPEO_n$ degradation. The results revealed the important role of the glyoxylate cycle in $OPEO_n$ utilization by strain TX1.

MATERIALS AND METHODS

Bacterial strains and culture conditions. The bacterial strains and plasmids used in this study are listed in Table 1. Strain TX1 was routinely grown at 30°C in Luria-Bertani (LB) or minimal salt basal (MSB) medium with appropriate sources of carbon and energy (12). In liquid culture, cells were grown in a 50-ml culture volume in 250-ml Erlenmeyer flasks with shaking in an incubator at 180 rpm. For plate culture, agar was added at a final concentration of 1.5% (wt/vol). *Escherichia coli* was grown in LB medium at 37°C and served as the host organism for plasmid retention. Ampicillin (20 $\mu g \cdot ml^{-1}$), gentamicin (20 $\mu g \cdot ml^{-1}$), and kanamycin (20 $\mu g \cdot ml^{-1}$) were used to select the transformed *E. coli* or TX1 cells.

Plasmid and chromosomal DNA isolation. Total DNA and plasmid DNA were extracted using previously described procedures (19). For the PCR amplifications, a 50-μl PCR mixture, consisting of 0.2 mM each of the four dinucleoside triphosphates (dNTPs), 20 pmol each primer, 10 ng of extracted DNA, and 1.25 U of *Taq* DNA polymerase (Toyobo Co. Ltd., Japan), with an appropriate amount of reaction buffer, was used. Amplification was performed in a program temperature control system, PC-808 (Astec Co. Ltd.). Other molecular techniques were performed using standard procedures (20) or as recommended by the reagent suppliers. The oligonucleotide primers used in this study are listed in Table 2.

Transposon mutagenesis. The plasmid pRL27, which carries the transposon Tn*5* with a kanamycin (Km) resistance gene, was chosen as the vector for transferring the transposon to *P. nitroreducens* TX1. The introduction and subsequent transposition of the modified mini-Tn*5* transposon into the *P. nitroreducens* TX1 genome were carried out as previously described by mating TX1 and *E. coli* BW20767, which carries the transposon delivery vector pRL27 (21, 22). The donor BW20767(pRL27), the helper *E. coli* HB101(pRK2013), and the recipient strain TX1 were mixed at a ratio of 1:1:1, spotted on an LB agar plate, and cultured at 30°C for 12 h to allow conjugational transfer of the pRL27 plasmid into the recipient cells. Transconjugants were initially selected on MSB agar medium containing 0.5% succinate, ampicillin, and kanamycin. They were then subjected to $OPEO_n$ utilization screening as follows. First, single colonies were streaked on MSB agar containing 0.5% $OPEO_n$. The plates were then incubated in an inverted position for several days at 30°C. Mutant strains that did not show visible growth on the plate were designated $OPEO_n$-negative mutants and were then subjected to further study.

Plasmid rescue and recovery of interrupted genes. Larsen et al. have shown that one-step cloning of the transposon with its associated flanking DNA can be accomplished after mutation by pRL27 (21). The selected $OPEO_n$-negative mutants were grown overnight in LB plus kanamycin and ampicillin, and then 1.5 ml of each culture was transferred to microcentrifuge tubes. Next, the cells were harvested by centrifugation at 10,000 × *g* for 1 min. Chromosomal DNA was isolated from the pelleted cells as described above and digested with the restriction enzyme BamHI, which does not cut within the transposon sequence of pRL27. The digested DNA was cleaned, which was followed by self-ligation using the T4 ligase at 20°C for 1 h. Material from ligated mixtures was transformed into *E. coli* DH5α λpir, as previously described, and plated onto LB agar-kanamycin plates in order to select for cells transformed with the ligated pRL27 plasmid that also contained the flanking *P. nitroreducens* TX1 DNA (23). Next, the transposon with its flanking DNA was isolated using the Midi Plus ultrapure plasmid extraction system (Viogene, Taipei, Taiwan). Primers tpnRL17-1 and tpnRL13-2, which anneal to positions within the transposon sequence in pRL27 and read outwards into flanking DNA regions, were used for sequencing (21). Sequencing of the DNA interrupted by the transposon was carried out on an automatic genetic analyzer (Applied Biosystems). The genes disrupted by the transposon were identified using the BioEdit software by a local BLAST search against the TX1 draft genome sequence and also against the GenBank database.

In-frame deletion mutagenesis. Four genes (*aceA*, *aceB*, *fixC*, and *glcE*, which encode isocitrate lyase, malate synthase, dehydrogenase, and glycolate dehydrogenase, respectively) were inactivated by in-frame deletion to avoid any polar effect. The in-frame *aceA* deletion mutant of strain TX1 was constructed by allelic replacement, as previously described (24). A gene fragment containing about a 98% deletion of the internal region of *aceA* was created by overlap extension PCR, as described previously (25). The primers used were Ace_FEco, Ace_RXho, Ace_FXho, and Ace_RHind. The internally deleted gene fragment was cloned into a suicide vector (pK18mobsacB), which was named pKaceA. The *aceA* deletion mutant of TX1 was created by triple mating between strains TX1, *E. coli* DH5α(pKaceA), and *E. coli* HB101(pRK2013). The TX1 Δ*aceA* strain was screened as described previously (24) and confirmed by PCR. The same procedure was applied to construct the TX1 Δ*aceB*, TX1 Δ*fixC*, and TX1 Δ*glcE* mutants using the primers that are described in Table 2.

TABLE 1 Bacterial strains and plasmids used in this study

Strain or plasmid	Description[a]	Reference or source
Strains		
Pseudomonas nitroreducens		
TX1	Wild-type strain TX1, Amp^r	Laboratory collection
Δ*aceA* mutant	Strain TX1 with in-frame deletion of *aceA* gene, Amp^r	This study
Δ*aceB* mutant	Strain TX1 with in-frame deletion of *aceB* gene, Amp^r	This study
Δ*fixC* mutant	Strain TX1 with in-frame deletion of *fixC* gene, Amp^r	This study
Δ*glcE* mutant	Strain TX1 with in-frame deletion of *glcE* gene, Amp^r	This study
Δ*aceA*(pBaceA) mutant	Δ*aceA* mutant harboring plasmid pBaceA, Amp^r, Gm^r	This study
Δ*aceB*(pBaceB) mutant	Δ*aceB* mutant harboring plasmid pBaceB, Amp^r, Gm^r	This study
E. coli		
DH5α	F^- ϕ80d*lacZ*ΔM15 Δ(*lacZYA-argF*)*U169 deoR recA1 endA1 hsdR17*(r_K^- m_K^+) *phoA supE44* λ^- *thi-1 gyrA96*	Laboratory collection
DH5α/λpir	λpir lysogen of DH5α	Laboratory collection
BW20767	Containing pRL27; used as donor for pRL27 conjugations	Larsen et al. (21)
HB101	Containing pRK2013; used as helper for pRL27 conjugations	Figurski and Helinski (22)
Plasmids		
pGEM-T Easy	PCR cloning vector, Amp^r	Promega
pGaceA	Amp^r, pGEM-T Easy with 2.6-kb fragment, including *aceA*	This study
pGaceB	Amp^r, pGEM-T Easy with 3.2-kb fragment, including *aceB*	This study
pRL27	Km^r, mini-Tn*5* transposon (*ori*R6K) delivery vector	Larsen et al. (21)
pRK2013	Km^r, carrying RK2 transfer genes	Figurski and Helinski (22)
pK18mobsacB	Km^r, *oriT*(RP4) *sacB lacZ*α Plac Pmbi, mobilization and counterselection	Schafer et al. (24)
pKaceA	pK18mob*sacB* containing a gene fragment with 98% deletion of internal region of *aceA*	This study
pKaceB	pK18mob*sacB* containing a gene fragment with 98% deletion of internal region of *aceB*	This study
pKfixC	pK18mob*sacB* containing a gene fragment with 98% deletion of internal region of *fixC*	This study
pKglcE	pK18mob*sacB* containing a gene fragment with 98% deletion of internal region of *glcE* (GenBank accession no. WP_017520229.1)	This study
pBBR1MCS-5	Broad-host-range cloning vector, *lacZ*, Gm^r	Kovach et al. (26)
pBaceA	Gm^r, pBBR1-MCS5 with 2.6-kb fragment, including *aceA*	This study
pBaceB	Gm^r, pBBR1-MCS5 with 3.2-kb fragment, including *aceB*	This study
pBglcE	Gm^r, pBBR1-MCS5 with 1.5-kb fragment, including *glcE*	This study

[a] Km^r, Gm^r, and Amp^r indicate resistance to kanamycin, gentamicin, and ampicillin, respectively.

Complementation of the TX1 Δ*aceA*, TX1 Δ*aceB*, and TX1 Δ*glcE* mutants. To determine whether the $OPEO_n$ utilization deficiency was due to an inactivated gene, the TX1 Δ*aceA*, TX1 Δ*aceB*, and TX1 Δ*glcE* mutants were complemented with appropriate wild-type genes expressed in a broad-host-range vector pBBR1MCS5 (26). For example, the *aceA* expression vector was constructed as follows: a PCR fragment (2.6 kb) obtained by amplifying the chromosomal DNA of TX1 with the primers aceA(f)_F and aceA(f)_R was ligated into a pGEM-T Easy vector (Promega Co.). The resulting vector (pGaceA) was then amplified in *E. coli* DH5α, purified, and digested with EcoRI and HindIII to generate the PCR product. Next, the retrieved PCR-amplified fragment was ligated into pBBR1MCS-5, which had been cut with the same restriction enzymes. The resulting plasmid (pBaceA) was then introduced into TX Δ*aceA* by conjugation using the helper strain *E. coli* HB101(pRK2013). The presence of the intact *aceA* gene was confirmed by DNA sequencing. The recombinant TX1 Δ*aceA*(pBaceA) strain was selected on MSB agar containing 0.5% $OPEO_n$, ampicillin, and gentamicin. The same procedure was applied for complementation of the TX1 Δ*aceB* and TX1 Δ*glcE* mutants with pBaceB and pBglcE, respectively, which were constructed using the primers listed in Table 2.

Preparation of crude cell extract from strain TX1. A 0.5-liter culture of TX1 grown on either 0.5% $OPEO_n$-MSB or 0.5% succinate-MSB was used for the preparation of crude cell extract. The cells were collected by centrifugation (11,000 × *g*, 10 min, 4°C), washed with 10 mM potassium phosphate buffer (pH 7.0), and suspended in 5 ml of the same buffer. The cell suspension was subjected to sonication for 3 min with 50% pulse on ice using the Sonicator 4000 (Misonix, Farmingdale, NY) to disrupt the cells (27). In the process of cell lysis, 0.15 mM protease inhibitor (phenylmethylsulfonyl fluoride) was added. After the removal of unbroken cells and cell debris by centrifugation (11,000 × *g*, 10 min, 4°C), the supernatant was collected by ultracentrifugation (200,000 × *g*, 1 h, 4°C) and used as the crude cell extract. Protein concentrations were determined using the Bradford protein assay with bovine serum albumin as the standard.

Enzyme assays. The acetaldehyde dehydrogenase activity assay was performed by measuring the rate of appearance of NADH at 340 nm in 1-cm-path cuvette at 25°C with a Beckman DU640 spectrophotometer (Beckman Coulter, Krefeld, Germany). The incubation mixtures contained the following constituents in a final volume of 1 ml: 10 mM potassium phosphate buffer (pH 7.0), 10 mM 2-mercaptoethanol, 2 mM NAD^+, 0.5 mg of cell crude extract, and 1 mM acetaldehyde. The reaction was started by the addition of acetaldehyde. For isocitrate lyase activity, a spectrophotometric assay was used to measure isocitrate-dependent formation of glyoxylate. The standard reaction mixture (0.5 ml) contained 10 mM potassium phosphate buffer (pH 7.0), 5 mM $MgCl_2$, 2 mM dithioerythritol, 3.5 mM phenylhydrazine, and 0.5 mg of cell crude extract. The reactions were started by the addition of 2 mM isocitrate, and the formation of the glyoxylate phenylhydrazone derivative was monitored at 324 nm. Malate synthase activity in the crude cell extracts was measured by the method of Srere et al. by tracking the glyoxylate- and acetyl-CoA-dependent release of CoA (28). Acetyl-CoA synthetase activity in the crude cell extracts was measured in the presence of ATP, acetate, and CoA, as described in a previous study (29).

RESULTS AND DISCUSSION

Transposon mutagenesis of *P. nitroreducens* TX1. The availability of the draft genome sequence of *P. nitroreducens* TX1 provides

TABLE 2 Oligonucleotide primers used in this study

Primer name	Sequence (5′–3′)[a]	Note	Restriction site	Reference or source
tpnRL17-1	AACAAGCCAGGGATGTAACG	For sequencing of transposon insertion		Larsen et al. (21)
tpnRL13-2	CAGCAACACCTTCTTCACGA			Larsen et al. (21)
AceA_FEco	GCGAATTCACGTGCTCGACTAAGCCTTC	For in-frame deletion of *aceA* in TX1	EcoRI	This study
AceA_RXho	GCCTCGAGTGCGGACATGGCCAATCCTTC		XhoI	This study
AceA_FXho	GCCTCGAGTTCCACTAAGAACTGGCTCAC		XhoI	This study
AceA_RHind	GCAAGCTTCTCTTGATCAGCGGCAGTTT		HindIII	This study
AceB_FEco	GCGAATTCGAAGCGAAGAACGGGTACAG	For in-frame deletion of *aceB* in TX1	EcoRI	This study
AceB_RXho	GCCTCGAGTTCAGTCATTGCTTGCCTCAC		XhoI	This study
AceB_FXho	GCCTCGAGGGTCTGTAAGCACCTCGCGCC		XhoI	This study
AceB_RHind	GCAAGCTTAACCGTCTGCAGTCTTTCTGA		HindIII	This study
FixC_FEco	GCGAATTCCAGTGATCCGTCGAAGGTG	For in-frame deletion of *fixC* in TX1	EcoRI	This study
FixC_RSma	GCCCCGGGGGCGGGCATCAGAAGGGCTCC		SmaI	This study
FixC_FSma	GCCCCGGGGCCAGCTGAATAGGACAAGG		SmaI	This study
FixC_RHind	GCAAGCTTCAGTTCAGCTCCACCTCGAT		HindIII	This study
GlcE_FEco	GCGAATTCAGTTTCGATTCGGTGGAAAA	For in-frame deletion of *glcE* in TX1	EcoRI	This study
GlcE_RXho	GCCTCGAGATCGGCCATCAGAAACGCTCC		SmaI	This study
GlcE_FXho	GCCTCGAGGAGCTCTGATGCAAACCAACC		SmaI	This study
GlcE_RHind	GCAAGCTTCGTCTGCACTATGGCTTCG		HindIII	This study
aceA(f)_F	GCGAATTCACGTGCTCGACTAAGCCTTC	For construction of pBaceA	EcoRI	This study
aceA(f)_R	GCAAGCTTCTCTTGATCAGCGGCAGTTT		HindIII	This study
aceB(f)_F	GCGAATTCGAAGCGAAGAACGGGTACAG	For construction of pBaceB	EcoRI	This study
aceB(f)_R	GCAAGCTTAACCGTCTGCAGTCTTTCTGA		HindIII	This study
glcE(f)_F	TGCCCGGGGAGCTGGAACGCGCCG	For construction of pBglcE	SmaI	This study
glcE(f)_R	GCACAAGCTTGATCAGGTAGATGCGCC		HindIII	This study

[a] Restriction enzyme sites are underlined.

an opportunity for investigating genes that play significant roles in $OPEO_n$ utilization (18). In order to identify genes involved in $OPEO_n$ catabolism, the Tn*5* vector pRL27 (21), which has been used widely in *Pseudomonas* genetics, was used to construct a mutant library of strain TX1, as described in Materials and Methods. In total, 30,000 Tn*5* insertion mutants of TX1 were successfully obtained. After 48 h of incubation at 30°C, these mutants were screened, and 93 (0.31%) of them failed to grow on 0.5% $OPEO_n$-MSB but still grew on 0.5% succinate-MSB.

A total of 6,341 open reading frames (ORFs) have been putatively identified in the TX1 draft genome (18), and therefore, the Tn*5* mutant library would seem to have 4.7× ORF coverage of the TX1 genome. The stability of the Tn*5* transposon in the transformants was also tested using two of the mutants (C94-4 and A16-7). After 10 generations of the single-colony propagation by subculture on LB plates, the initial and final colonies were found to still retain the kanamycin resistance and, in addition, the Tn*5* transposon had remained in the same genomic position on the genome, with this being determined by PCR. These findings confirm that the transposon insertion events present in the transformants from this library are stable.

The transposon insertion points of the 93 mutants defective in $OPEO_n$ utilization were identified by the plasmid rescue, followed by nucleotide sequencing using a transposon-derived primer set (21). The insertion loci harboring Tn*5* were then mapped to 42 independent coding genes, three noncoding sequences, and one 23S rRNA. These results are summarized in Table 3. Of these 42 genes, 11 had been mutated multiple times to give a number of different mutant strains for a given specific gene. These were the *dedA* gene, which had 12 mutants; the *hit* gene, with 11 mutants; the *aceB* gene, with seven mutants; the *aceA* and *rfaG* genes, with six mutants; the *rfe* gene, with four mutants; the *coq7* gene and a gene encoding a hypothetical protein, with three mutants; and the *yfgC* and *fixC* genes and a gene encoding a transcriptional regulator, with two mutants (Table 3). These genes with multiple mutations were used for further investigation. Among these 42 disrupted genes, 39 genes could be located within the draft genome of TX1 (accession no. AMZB01000000), while the other three genes, namely, those of the K11-8, C2-42, and T43-26 mutants, were found to be similar to genes present in the genomes of other strains, including *Mycobacterium abscessus*, *Comamonas testosteroni*, and *Pseudomonas knackmussii* (accession numbers WP_049232543, WP_003060809, and WP_043252236.1, respectively), but not within the draft genome of TX1 (18).

Functional characterization of the mutant genes. The proteins encoded by the 42 unique genes identified in this study ($OPEO_n$ growth-associated proteins) were grouped into functional classes using the clusters of orthologous groups (COG), as shown in Table 3. When this was done, six proteins (14.3%) were classified into the information storage- and processing-related categories (K and L). Furthermore, the cellular process- and signaling-related categories (O, M, N, T, and V) consisted of 12 proteins (28.6%). Fifteen proteins (35.7%) were present in the metabolism-related categories (C, G, E, F, H, and I). Two poorly characterized COG groups (R and S) were found to contain six proteins (14.3%). In addition, for the category "no related COGs" (the protein is not predicted to belong to any of the currently defined COGs), there were found to be three proteins (7.1%).

Overall, 12 (28.5%) genes were predicted to encode catabolic enzymes. Three proteins (isocitrate lyase, malate synthase, and FixC dehydrogenase) are known to be involved in energy production and conversion, whereas nine proteins (diadenosine tetra-

TABLE 3 Characterization of the $OPEO_n$-negative mutants of *P. nitroreducens* TX1 obtained by Tn*5* insertional mutagenesis

Mutant[a]	Gene	Function[b]	Protein accession no.	Function group (COGs)[c]
C94-4, C100-12, N8-29, N10-35, N36-50, P30-12	*aceA*	Isocitrate lyase	WP_017517106.1	COG2224C
A16-7, C87-31, C90-8, K1-02, N38-2, P10-33, T16-15	*aceB*	Malate synthase	WP_017520204.1	COG2225C
B1-31, B1-33	*fixC*	Dehydrogenase (flavoprotein)	WP_017520493.1	COG0644C
A2-42	*hisP*	ABC-type histidine transport system	WP_017517948.1	COG4598E
C39-17	*gdh2*	NAD-specific glutamate dehydrogenase	WP_017519332.1	COG2902E
C96-34	*rhtB*	Putative threonine efflux protein	WP_017521173.1	COG1280E
T8-50	*ilvB*	Thiamine pyrophosphate-requiring enzyme	WP_017516325.1	COG0028EH
N43-34	*putP*	Na^+/proline symporter	WP_017518917.1	COG0591ER
C48-18, C77-4, C95-33, P19-3, P19-32, P38-47, P42-36, T10-24, T15-48, T57-1, T58-5	*hit*	Diadenosine tetraphosphate hydrolase and other HIT family hydrolases	WP_017517344.1	COG0537FGR
B3-49	*bglX*	Beta-glucosidase-related glycosidase	WP_017517232.1	COG1472G
P40-18	*zwf*	Glucose-6-phosphate 1-dehydrogenase	WP_017520335.1	COG0364G
K32-8	*gshA*	Gamma-glutamylcysteine synthetase	WP_017520855.1	COG2918H
A21-39	*ubiE*	Methylase involved in ubiquinone biosynthesis	WP_017521165.1	COG2226H
C73-29, C97-46, P24-25	*coq7*	Demethoxyubiquinone hydroxylase	WP_017517343.1	COG2941H
B3-29	*fadB*	3-Hydroxyacyl-CoA dehydrogenase	WP_017519287.1	COG1250I
A11-1	*yafY*	Predicted transcriptional regulator	WP_017518996.1	COG2378K
C4-30	*araC*	AraC-type DNA-binding domain-containing protein	WP_017521913.1	COG2207K
B5-50	*aRO8*	Transcriptional regulator	WP_017518869.1	COG1167KE
C15-19	*hepA*	Superfamily II DNA/RNA helicase	WP_017522209.1	COG0553KL
K11-8	*dob10*	DEAD/DEAH box helicase	WP_049232543	COG4581L
C2-42	Tn*3*	Transposase	WP_003060809	COG1961L
C82-3, T44-10, T45-21, T67-19, T78-50, T77-39	*rfaG*	Glycosyltransferase	WP_017520449.1	COG0438 M
C85-47, T41-40, T66-4, T66-19	*rfe*	UDP-*N*-acetylglucosamine-1-phosphate transferase	WP_017520347.1	COG0472 M
N52-26	*gt2*	Glycosyltransferases	WP_017520448.1	COG1216 M
P33-4	*nlpD*	Membrane protein related to metalloendopeptidase	WP_017517352.1	COG0739 M
P55-13	*wcaA*	Glycosyltransferase involved in cell wall biogenesis	WP_017517134.1	COG0463 M
T43-26	*galU*	UTP-glucose-1-phosphate uridylyltransferase	WP_043252236.1	COG1210 M
B7-14	*wcaG*	Nucleoside diphosphate-sugar epimerase	WP_017520346.1	COG0451MG
B6-16	*tar*	Methyl-accepting chemotaxis protein	WP_017516259.1	COG0840NT
N24-8	*anmK*	Predicted molecular chaperone	WP_017517351.1	COG2377O
A21-12	COG4590	ABC-type uncharacterized transport system	WP_017520681.1	COG4590R
A7-47	*ybcL*	Membrane-bound metal-dependent hydrolase	WP_017520412.1	COG1988R
B2-48, B7-43	*yfgC*	Putative Zn-dependent protease	WP_017519734.1	COG4783R
K17-10	*roxA*	Ribosomal protein L16 Arg81 hydroxylase	WP_017517102.1	COG2850S
K21-12	*tauE*	Cytochrome biogenesis protein	WP_017516824.1	COG2836S
C3-45, C5-33, C9-50, C61-29, C63-28, C64-38, P32-21, P33-22, T11-1, T15-44, T17-21, T46-48	*dedA*	Membrane protein	WP_017521718.1	COG0586S
N30-8	*atoC*	Response regulator	WP_017518918.1	COG2204T
P36-32	*GGDEF*	GGDEF domain, diguanylate cyclase	WP_017517199.1	COG2199T
C12-38	*norM*	Na^+-driven multidrug efflux pump	WP_017518643.1	COG0534V
B3-46, B4-25		Transcriptional regulator	WP_017516487.1	NC
C11-3, T56-25, T57-21		Hypothetical protein	WP_017520115.1	NC
A28-42		Hypothetical protein	WP_017520049.1	NC
T12-28		23S rRNA		NC
A6-49		Noncoding sequence		NC
B2-47		Noncoding sequence		NC
P34-24		Noncoding sequence		NC

[a] The representative strains (in bold) were selected for further investigation, as described in the text.
[b] HIT, histidine triad.
[c] The proteins were classified into functional categories according to the clusters of orthologous groups (COG). The functional categories are information storage and processing, including COG categories K (transcription) and L (replication, recombination, and repair); cellular processes and signaling, including O (posttranslational modification, protein turnover, and chaperones), M (cell wall/membrane/envelope biogenesis), N (cell motility), T (signal transduction mechanisms), and V (defense mechanisms); metabolism, including C (energy production and conversion), G (carbohydrate transport and metabolism), E (amino acid transport and metabolism), F (nucleotide transport and metabolism), H (coenzyme transport and metabolism), and I (lipid transport and metabolism); poorly characterized, including R (general function prediction only) and S (function unknown). NC, proteins not classified into a COG.

phosphate hydrolase, NAD^+-specific glutamate dehydrogenase, thiamine pyrophosphate-requiring enzyme, β-glucosidase-related glycosidase, glucose-6-phosphate 1-dehydrogenase, γ-glutamylcysteine synthetase, UbiE methylase involved in ubiquinone biosynthesis, demethoxyubiquinone hydroxylase, and 3-hydroxyacyl-CoA dehydrogenase) are known to be involved in the metabolism of amino acids, carbohydrates, coenzymes, and lipids. Of these, diadenosine tetraphosphate hydrolase (*hit*) is a key en-

zyme controlling the *in vivo* concentration of the dinucleotide diadenosine tetraphosphate that has been proposed to play a range of roles in processes, such as control of DNA replication and repair, signaling in stress response, and apoptosis (30).

$OPEO_n$ is one of the most widely used nonionic surfactants; it is used in biology to lyse cells to allow the extraction of protein and other cellular organelles. Previous studies have suggested that $OPEO_n$ affects the cell membrane by disrupting its structural integrity and functioning, which results in increased membrane fluidity and permeabilization (31). In our previous work, we found that *P. nitroreducens* TX1 is able to tolerate up to 20% $OPEO_n$ in MSB medium. Therefore, the membrane of TX1 might have special structural features that allow $OPEO_n$ to be tolerated. In this context, it should be noted that seven (16.6%) out of the 42 identified proteins, namely, three glycosyltransferases (*rfaG*, *gt2*, and *wcaA*), a UDP-*N*-acetylglucosamine-1-phosphate transferase (*rfe*), a membrane protein related to metalloendopeptidase (*nlpD*), a UTP-glucose-1-phosphate uridylyltransferase (*galU*), and a nucleoside-diphosphate-sugar epimerase (*wcaG*), are known to be linked to cell wall/membrane/envelope biogenesis. For example, the deletion of *ssg*, which encodes a glycosyltransferase in *Pseudomonas alkylphenolia* KL28, has been shown to cause the loss of lipopolysaccharide O antigen, which alters the composition of the exopolysaccharide. Furthermore, this mutant strain was found to have reduced surface spreading, reduced pellicle formation, and reduced biofilm formation; these were probably due to the cumulative effects of lipopolysaccharide truncation and alterations to the cell's exopolysaccharide composition (23). In some bacterial species, UDP-*N*-acetylglucosamine-1-phosphate transferase has been shown to play an important role in the biosynthesis of various polymers within the bacterial cell wall, such as common antigen and lipopolysaccharide O antigen (32). UTP-glucose-1-phosphate uridylyltransferase is an enzyme associated with glycogenesis. This enzyme synthesizes UDP-glucose from glucose-1-phosphate. UDP-glucose has been reported to be involved in galactose utilization, in glycogen synthesis, and in the synthesis of various carbohydrate moieties, such as glycolipids, glycoproteins, and proteoglycans (33). Interestingly, *yfgC* codes for a putative Zn-dependent protease, and although its function is unknown, the chemical and genetic data suggest that it also plays a role in outer membrane protein biogenesis (34). Furthermore, five (11.9%) out of the 42 genes were predicted to encode transport proteins, among which two ABC transporters were identified. Such transport proteins were likely to play important roles in the transport of $OPEO_n$ into the cell. For the functions of the DedA membrane protein, the recent genetic approaches have revealed important roles in membrane homeostasis. Bacterial DedA family mutants display such intriguing phenotypes as cell division defects, temperature sensitivity, altered membrane lipid composition, elevated envelope-related stress responses, and loss of proton motive force (35). Finally, there are a significant number of mutants that fall within the hypothetical, unknown, and unclassified gene categories, which suggests that there is still a large number of unknown genes across the *P. nitroreducens* genome potentially involved in $OPEO_n$ metabolism that remain to be explored, including the three not found in the TX1 draft genome. Further studies on these genes using complementation and other strategies will improve our understanding of the strain TX1 and its tolerance and degradation of $OPEO_n$.

Role of the glyoxylate cycle in $OPEO_n$ degradation by TX1. Isocitrate lyase and malate synthase, which are both key enzymes in the glyoxylate cycle, were frequently detected during screening of mutants unable to grow on 0.5% $OPEO_n$. In the glyoxylate cycle, two molecules of acetyl-CoA are converted into oxaloacetate, thus bypassing the reactions of the tricarboxylic acid (TCA) cycle in which CO_2 is released. The glyoxylate cycle is essential when cells are growing on C_2 compounds, because this pathway allows the synthesis of all cellular compounds with three or more carbon atoms; examples include the biosynthesis of amino acids and nucleotides. To confirm the role of these two enzymes in $OPEO_n$ utilization, in-frame deletion mutants lacking the *aceA* and *aceB* genes were created from strain TX1. As expected from the transposon mutagenesis results, the TX1 Δ*aceA* and TX1 Δ*aceB* mutants were unable to grow on $OPEO_n$. The in-frame deletion mutants were then used for complementation analysis. Two plasmids, pBaceA and pBaceB, which carry the *aceA* and *aceB* genes, respectively, were constructed and transferred independently from *E. coli* into the TX1 Δ*aceA* and TX1 Δ*aceB* mutant strains by conjugation. In both cases, the introduction of the wild-type copy of the gene resulted in a return to the wild-type growth pattern, confirming the role of the *aceA* and *aceB* in $OPEO_n$ utilization. In addition, isocitrate lyase and malate synthase activities in cell extract of wild-type cells grown on $OPEO_n$ were 277.6 ± 5 (mean ± standard deviation) and 15.1 ± 5 nmol · min^{-1} · mg^{-1}, respectively. These activities were downregulated 8.8- and 1.7-fold in cells grown on succinate (31.3 ± 6.5 and 8.7 ± 2 nmol · min^{-1} · mg^{-1}, respectively). These results clearly reveal that the glyoxylate cycle plays a critical role in $OPEO_n$ degradation by strain TX1.

Growth of the mutants on different carbon sources. Eleven mutants (TX1 Δ*aceA*, TX1 Δ*aceB*, TX1 Δ*fixC*, C48-18, C73-29, C82-3, C85-47, B2-48, C3-45, B3-46, and C11-3), which are representatives of the 11 genes present in the Tn*5* library as multiple events, TX1 Δ*glcE*, and the three complemented strains [TX1 Δ*aceA*(pBaceA), TX1 Δ*aceB*(pBaceB), and TX1 Δ*glcE*(pBglcE)] were tested for their growth on 0.1% $OPEO_n$, 0.1% $NPEO_n$, 0.1% dodecyl octaethoxylate (AEO_8), 0.1% ethanol, 0.1% acetate, 0.1% glycolate, or 0.1% pyruvate as the sole source of carbon (Table 4). The *glcE* gene was deleted to test the cleavage of $OPEO_n$ by terminal carboxylation, followed by hydrolysis to yield glycolate in strain TX1 (Fig. 1, oxidation). Wild-type TX1 is unable to grow on polyethylene glycol 400 (PEG 400), polyethylene glycol 1000 (PEG 1000), acetaldehyde, or glyoxylate; therefore, these compounds were not used for growth testing of the mutants. The generation time of wild-type TX1 was much longer when grown on glycolate (10.8 to 11.8 h) than on $OPEO_n$, $NPEO_n$, AEO_8, ethanol, acetate, or pyruvate (1.5 to 4.8 h) (Table 4). All mutants were able to grow on pyruvate, with generation times ranging from 3.6 to 4 h. When $NPEO_n$ or AEO_8 was used as the sole source of carbon, five mutants, TX1 Δ*fixC*, TX1 Δ*glcE*, TX1 Δ*aceA*(pBaceA), TX1 Δ*aceB*(pBaceB), and TX1 Δ*glcE*(pBglcE), showed growth on these compounds, with generation times ranging from 1.5 to 3.7 h, whereas the rest of mutants failed to grow at all. When ethanol or acetate was used as the sole source of carbon, the two glyoxylate cycle mutants (TX1 Δ*aceA* and TX1 Δ*aceB*) failed to grow, but others were able to grow on ethanol or acetate, with generation times ranging from 2.7 to 4.8 h. In addition, the two mutants TX1 Δ*aceB* and TX1 Δ*glcE* failed to grow on 0.1% glycolate, but the

TABLE 4 Growth of TX1 mutants on various carbon sources

Strain[a]	Description	Generation time (mean ± SD) (h)[b]						
		$OPEO_n$	$NPEO_n$	AEO_8	Ethanol	Acetate	Pyruvate	Glycolate
TX1	Wild type	1.5 ± 0.1	3.2 ± 0.1	3.7 ± 0.2	4.8 ± 0.2	2.7 ± 0.2	3.6 ± 0.4	11.3 ± 3.1
TX1 Δ*aceA*	Deletion of isocitrate lyase gene	−	−	−	−	−	3.6 ± 0.4	11.5 ± 2.5
TX1 Δ*aceB*	Deletion of malate synthase gene	−	−	−	−	−	3.6 ± 0.4	−
TX1 Δ*fixC*	Deletion of dehydrogenase gene	1.5 ± 0.1	3.1 ± 0.1	3.7 ± 0.1	4.8 ± 0.2	2.7 ± 0.2	3.6 ± 0.4	10.8 ± 2.2
TX1 Δ*glcE*	Deletion of glycolate dehydrogenase gene	1.5 ± 0.1	3.2 ± 0.1	3.7 ± 0.1	4.7 ± 0.1	2.9 ± 0.3	4 ± 0.2	−
C48-18	Mutation at diadenosine tetraphosphate hydrolase gene	−	−	−	4.7 ± 0.2	2.7 ± 0.2	4 ± 0.2	11.2 ± 4.2
C73-29	Mutation at demethoxyubiquinone hydroxylase gene	−	−	−	4.7 ± 0.2	2.7 ± 0.2	4 ± 0.2	11.3 ± 3.3
C82-3	Mutation at glycosyltransferase gene	−	−	−	4.7 ± 0.2	2.9 ± 0.3	4 ± 0.2	11.5 ± 2.8
C85-47	Mutation at UDP-*N*-acetylglucosamine-1-phosphate transferase gene	−	−	−	4.7 ± 0.1	2.7 ± 0.2	4 ± 0.2	11.7 ± 2.5
B2-48	Mutation at putative Zn-dependent protease gene	−	−	−	4.8 ± 0.2	2.9 ± 0.3	4 ± 0.2	10.9 ± 3.2
C3-45	Mutation at gene encoding membrane protein	−	−	−	4.7 ± 0.2	2.9 ± 0.3	4 ± 0.2	11.6 ± 2.7
B3-46	Mutation at gene encoding transcriptional regulator	−	−	−	4.8 ± 0.1	2.9 ± 0.3	4 ± 0.2	11.8 ± 2.8
C11-3	Mutation at gene encoding unknown protein	−	−	−	4.7 ± 0.1	2.9 ± 0.3	4 ± 0.2	11.7 ± 3.1
TX1 Δ*aceA*(pBaceA)	Complementation of isocitrate lyase gene	1.5 ± 0.1	3.2 ± 0.1	3.6 ± 0.2	4.7 ± 0.1	2.9 ± 0.3	4 ± 0.2	11.1 ± 3.2
TX1 Δ*aceB*(pBaceB)	Complementation of malate synthase gene	1.5 ± 0.1	3.1 ± 0.1	3.7 ± 0.1	4.7 ± 0.2	2.9 ± 0.3	4 ± 0.2	10.8 ± 2.6
TX1 Δ*glcE*(pBglcE)	Complementation of glycolate dehydrogenase gene	1.5 ± 0.1	3.1 ± 0.1	3.7 ± 0.1	4.8 ± 0.2	2.9 ± 0.3	4 ± 0.2	11.2 ± 2.8

[a] Each strain was cultured in 5 ml of MSB plus 0.1% of the relevant carbon source.
[b] −, no growth; $OPEO_n$, Triton X-100; $NPEO_n$, Triton N-101; AEO_8, dodecyl octaethoxylate. Data are the results from three independent experiments.

other mutants were able to grow on it, with generation times ranging from 10.8 to 11.8 h.

Proposed mechanism for the degradation of $OPEO_n$ by *P. nitroreducens* TX1. The biodegradation of long-chain $APEO_n$ has been studied using isolated bacterial strains that grow solely on $OPEO_n$ or $NPEO_n$. Most isolates are from the genus *Pseudomonas*, which belongs to the *Gammaproteobacteria* (9, 13, 14). Based on the results of metabolite analyses, the initial degradation reaction of $APEO_n$ has been found to be a shortening of the ethoxylate chain by exoscission of the EO chains from the hydroxyl terminal side (13, 14, 16) (Fig. 1). Our group isolated *Pseudomonas* strain TX1, which has the ability to grow on $OPEO_n$ at a wide range of concentrations (9). LC-MS analysis of the intermediate metabolites revealed the presence of a gradual shortening process that affected the EO chains during $OPEO_n$ utilization. The results suggested that the same exo-type biodegradation process is occurring in TX1 as in other isolates.

The terminal oxidation model for the biodegradation of PEG under aerobic conditions has been reviewed previously (36, 37). In this model, the biodegradation of the PEG molecules is initiated through the oxidation of the terminal EO unit to a carboxyl group, which is followed by the liberation of glycolate. The carboxyl is converted to glyoxylate by glycolate dehydrogenase (GlcE). Tasaki et al. (38) isolated the *adh1* gene from *P. putida* S-5 and expressed this gene in *E. coli*. By measuring the reduction of 2,6-dichlorophenolindophenol (DCPIP) spectrophotometrically at 600 nm using a cell crude extract, alcohol dehydrogenase (Adh1) was shown to have activity against $OPEO_n$ of various EO chain lengths (38). However, its relevance to the ether cleavage step in $OPEO_n$ biodegradation remains unknown. The use of redox dye-based assay with crude extracts can be misleading, because crude cell extract may contain multiple activities that are able to utilize DCPIP as an electron acceptor (17). Furthermore, the detection of glycolate and an increase in GlcE activity have not been reported; such findings would support the terminal oxidation model. In our study, a *fixC* gene encoding a dehydrogenase was found among the mutants. However, an in-frame deletion mutant of the *fixC* gene retained the ability to grow on $OPEO_n$ in a manner similar to the wild type. These results suggest that the transposon insertion into *fixC* has a polar effect, and the *fixC* gene product itself may not play an important role in $OPEO_n$ utilization. In addition, TX1 grows only slowly on glycolate but does not grow at all on glyoxylate, PEG 400, or PEG 1000 as the sole source of carbon. In order to determine whether glycolic acid is involved in the metabolism of $OPEO_n$ by strain TX1, a *glcE* in-frame deletion mutant was constructed. As shown in Table 4, TX1 Δ*glcE* grew on $OPEO_n$ to a level comparable to that of the wild type. Interestingly, TX1 Δ*glcE* and TX1 Δ*aceB* were unable to grow on glycolate, whereas TX1 Δ*aceA* was able to grow. Interestingly, one isocitrate lyase gene was found in the TX1 genome (18). In addition, the isocitrate lyase activity in the cell extract of TX1 Δ*aceA* cells grown on glycolate or succinate was not detectable. These results suggest that the degradation of glycolate does not involve the glyoxylate cycle, because the isocitrate lyase mutant was able to grow on glycolate in a manner similar to the wild-type TX1 (Fig. 2). Considering the results, we conclude that the degradation of $OPEO_n$ by strain TX1 does not demonstrate an oxidative pathway involving the liberation of glycolate.

In the nonoxidative biodegradation model, biodegradation of the EO chain proceeds via the shift of a hydroxyl group, followed by the liberation of acetaldehyde, which is then quickly transformed to acetate by dehydrogenases that are ubiquitously distributed throughout the cell (39). The pathway for acetate degradation is well known and involves the conversion of acetate into acetyl-CoA, which then enters in the central carbon metabolism of the cell (39). In the glyoxylate cycle, the input of two molecules of acetyl-CoA results in a net synthesis of one molecule of succinate, which is then available for biosynthetic purposes (40). As shown in Table 4, TX1 was able to grow on either ethanol or acetate as the sole source of carbon, with generation times ranging from 2.7 to 4.8 h, but TX1 Δ*aceA* and TX1 Δ*aceB* were unable to grow on these carbon sources. These results suggest that the glyoxylate cycle plays a critical role in ethanol or acetate catabolism. The ethanol oxidation product acetate must first be activated to acetyl-CoA so it can be used as a carbon source and for the replenishment of intermediates within the TCA cycle; this would occur via the glyoxylate bypass in strain TX1. Our results suggest that nonoxidative biodegradation with the liberation of acetaldehyde is the

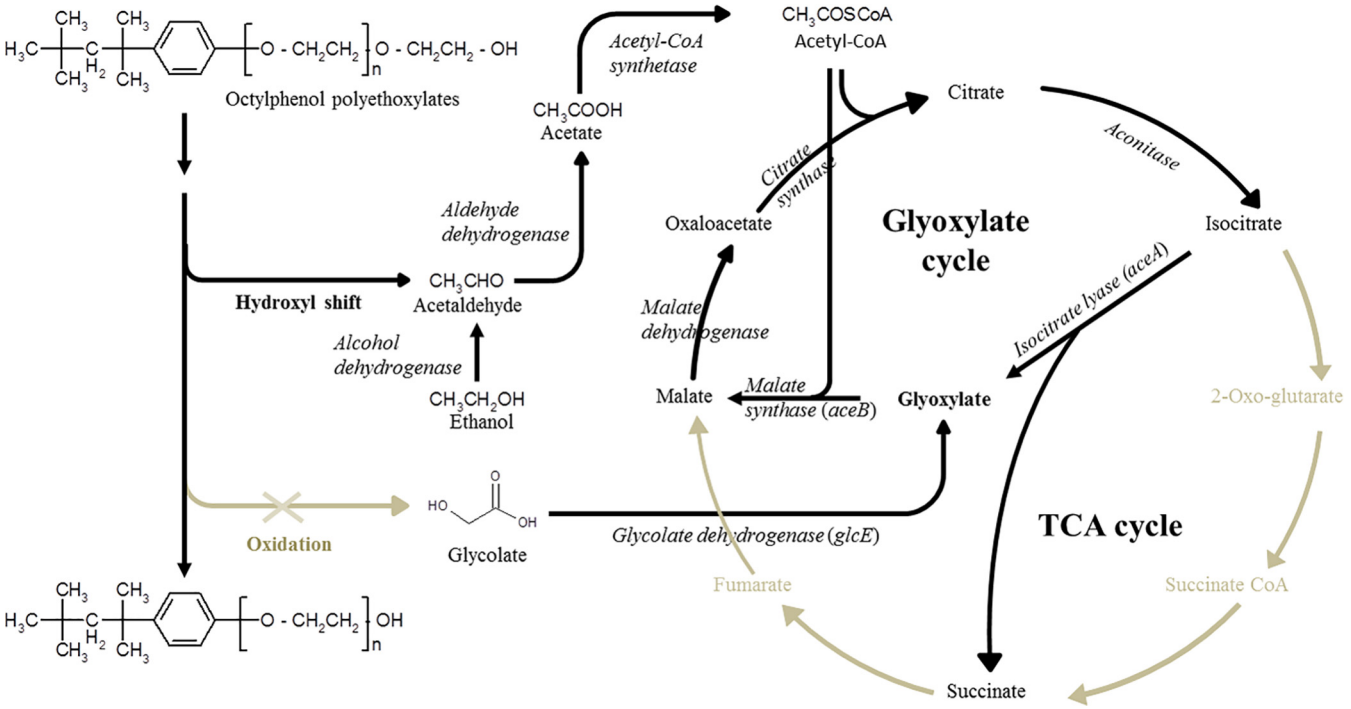

FIG 2 Proposed pathway and mechanism (black lines) for the degradation of $OPEO_n$ by *P. nitroreducens* TX1.

most likely pathway for $OPEO_n$ utilization in strain TX1 (Fig. 2). In addition, acetaldehyde dehydrogenase and acetyl-CoA synthetase activities were upregulated 13.1- and 2.1-fold in cells grown on $OPEO_n$ (211 ± 14 and 68.8 ± 1.1 nmol · min^{-1} · mg^{-1}, respectively) versus TX1 grown on succinate (16 ± 12 and 32.6 ± 1.2 nmol · min^{-1} · mg^{-1}, respectively). Further studies on the mechanism used for the liberation of acetaldehyde will be needed in order to improve our understanding of the degradation of $OPEO_n$ by strain TX1.

ACKNOWLEDGMENTS

This work was supported by the Ministry of Science and Technology, Taiwan (grant NSC102-2628-B-008-001-MY3) and the NRF-NSC cooperation program by the National Research Foundation of Korea (grant NRF-2013K2A1B8053138) and Ministry of Science and Technology, Taiwan (grant NSC 102-2923-B-008-001-MY2).

FUNDING INFORMATION

This work, including the efforts of Shir-Ly Huang, was funded by Ministry of Science and Technology, Taiwan (MOST) (NSC102-2628-B-008-001-MY3). This work, including the efforts of Shir-Ly Huang, was funded by Ministry of Science and Technology, Taiwan (MOST) (NSC 102-2923-B-008-001-MY2). This work, including the efforts of Kyoung Lee, was funded by National Research Foundation of Korea (NRF) (NRF-2013K2A1B8053138).

REFERENCES

1. **Chen HJ, Tseng DH, Huang SL.** 2005. Biodegradation of octylphenol polyethoxylate surfactant Triton X-100 by selected microorganisms. Bioresour Technol **96:**1483–1491. http://dx.doi.org/10.1016/j.biortech.2004.11.013.
2. **Saito I, Onuki A, Seto H.** 2004. Indoor air pollution by alkylphenols in Tokyo. Indoor Air **14:**325–332. http://dx.doi.org/10.1111/j.1600-0668.2004.00250.x.
3. **Pagano M, Lopez A, Volpe A, Mascolo G, Ciannarella R.** 2008. Oxidation of nonionic surfactants by Fenton and H_2O_2/UV processes. Environ Technol **29:**423–433. http://dx.doi.org/10.1080/09593330801983862.
4. **Giger W, Brunner PH, Schaffner C.** 1984. 4-Nonylphenol in sewage sludge: accumulation of toxic metabolites from nonionic surfactants. Science **225:**623–625. http://dx.doi.org/10.1126/science.6740328.
5. **Huang SL, Tuan NN, Lee K.** 2016. Occurrence, human intake and biodegradation of estrogen-like nonylphenols and octylphenols. Curr Drug Metab **17:**293–302. http://dx.doi.org/10.2174/1389200217666151210124821.
6. **Tanenbaum DM, Wang Y, Williams SP, Sigler PB.** 1998. Crystallographic comparison of the estrogen and progesterone receptor's ligand binding domains. Proc Natl Acad Sci U S A **95:**5998–6003. http://dx.doi.org/10.1073/pnas.95.11.5998.
7. **Sahambi SK, Pelland A, Cooke GM, Schrader T, Tardif R, Charbonneau M, Krishnan K, Haddad S, Cyr DG, Devine PJ.** 2010. Oral *p*-tert-octylphenol exposures induce minimal toxic or estrogenic effects in adult female Sprague-Dawley rats. J Toxicol Environ Health A **73:**607–622. http://dx.doi.org/10.1080/15287390903566682.
8. **Ying GG, Williams B, Kookana R.** 2002. Environmental fate of alkylphenols and alkylphenol ethoxylates—a review. Environ Int **28:**215–226. http://dx.doi.org/10.1016/S0160-4120(02)00017-X.
9. **Lin YW, Guo GL, Hsieh HC, Huang SL.** 2010. Growth of *Pseudomonas* sp. TX1 on a wide range of octylphenol polyethoxylate concentrations and the formation of dicarboxylated metabolites. Bioresour Technol **101:**2853–2859.
10. **Chen HJ, Guo GL, Tseng DH, Cheng CL, Huang SL.** 2006. Growth factors, kinetics and biodegradation mechanism associated with *Pseudomonas nitroreducens* TX1 grown on octylphenol polyethoxylates. J Environ Manage **80:**279–286. http://dx.doi.org/10.1016/j.jenvman.2005.09.009.
11. **Chen HJ, Huang SL, Tseng DH.** 2004. Aerobic biotransformation of octylphenol polyethoxylate surfactant in soil microcosms. Environ Technol **25:**201–210. http://dx.doi.org/10.1080/09593330409355453.
12. **Tuan NN, Hsieh HC, Lin YW, Huang SL.** 2011. Analysis of bacterial degradation pathways for long-chain alkylphenols involving phenol hydroxylase, alkylphenol monooxygenase and catechol dioxygenase genes. Bioresour Technol **102:**4232–4240. http://dx.doi.org/10.1016/j.biortech.2010.12.067.
13. **Nguyen MH, Sigoillot JC.** 1996. Isolation from coastal sea water and

characterization of bacterial strains involved in non-ionic surfactant degradation. Biodegradation **7:**369–375.
14. **John DM, White GF.** 1998. Mechanism for biotransformation of nonylphenol polyethoxylates to xenoestrogens in *Pseudomonas putida*. J Bacteriol **180:**4332–4338.
15. **Nishio E, Ichiki Y, Tamura H, Morita S, Watanabe K, Yoshikawa H.** 2002. Isolation of bacterial strains that produce the endocrine disruptor, octylphenol diethoxylates, in paddy fields. Biosci Biotechnol Biochem **66:**1792–1798. http://dx.doi.org/10.1271/bbb.66.1792.
16. **Maki H, Masuda N, Fujiwara Y, Ike M, Fujita M.** 1994. Degradation of alkylphenol ethoxylates by *Pseudomonas* sp. strain TR01. Appl Environ Microbiol **60:**2265–2271.
17. **White GF, Russell NJ, Tidswell EC.** 1996. Bacterial scission of ether bonds. Microbiol Rev **60:**216–232.
18. **Huang SL, Chen H, Hu A, Tuan NN, Yu CP.** 2014. Draft genome sequence of *Pseudomonas nitroreducens* strain TX1, which degrades nonionic surfactants and estrogen-like alkylphenols. Genome Announc **2**(1): e01262-13. http://dx.doi.org/10.1128/genomeA.01262-13.
19. **Ausubel FM, Brent R, Kingston RE, Moore DD, Seidman JG, Smith JA, Struhl K (ed).** 2003. Current protocols in molecular biology, ringbou ed. John Wiley & Sons, Charlottesville, VA.
20. **Sambrook J, Fritsch EF, Maniatis T.** 1989. Molecular cloning: a laboratory manual, 2nd ed. Cold Spring Harbor Laboratory Press, Cold Spring Harbor, NY.
21. **Larsen RA, Wilson MM, Guss AM, Metcalf WW.** 2002. Genetic analysis of pigment biosynthesis in *Xanthobacter autotrophicus* Py2 using a new, highly efficient transposon mutagenesis system that is functional in a wide variety of bacteria. Arch Microbiol **178:**193–201. http://dx.doi.org/10.1007/s00203-002-0442-2.
22. **Figurski DH, Helinski DR.** 1979. Replication of an origin-containing derivative of plasmid RK2 dependent on a plasmid function provided in trans. Proc Natl Acad Sci U S A **76:**1648–1652. http://dx.doi.org/10.1073/pnas.76.4.1648.
23. **Veeranagouda Y, Lee K, Cho AR, Cho K, Anderson EM, Lam JS.** 2011. Ssg, a putative glycosyltransferase, functions in lipo- and exopolysaccharide biosynthesis and cell surface-related properties in *Pseudomonas alkylphenolia.* FEMS Microbiol Lett **315:**38–45. http://dx.doi.org/10.1111/j.1574-6968.2010.02172.x.
24. **Schäfer A, Tauch A, Jager W, Kalinowski J, Thierbach G, Puhler A.** 1994. Small mobilizable multi-purpose cloning vectors derived from the *Escherichia coli* plasmids pK18 and pK19: selection of defined deletions in the chromosome of *Corynebacterium glutamicum*. Gene **145:**69–73. http://dx.doi.org/10.1016/0378-1119(94)90324-7.
25. **Ho SN, Hunt HD, Horton RM, Pullen JK, Pease LR.** 1989. Site-directed mutagenesis by overlap extension using the polymerase chain reaction. Gene **77:**51–59. http://dx.doi.org/10.1016/0378-1119(89)90358-2.
26. **Kovach ME, Elzer PH, Hill DS, Robertson GT, Farris MA, Roop RM, Jr, Peterson KM.** 1995. Four new derivatives of the broad-host-range cloning vector pBBR1MCS, carrying different antibiotic-resistance cassettes. Gene **166:**175–176. http://dx.doi.org/10.1016/0378-1119(95)00584-1.
27. **Tuan NN, Lin YW, Huang SL.** 2013. Catabolism of 4-alkylphenols by *Acinetobacter* sp. OP5: genetic organization of the *oph* gene cluster and characterization of alkylcatechol 2, 3-dioxygenase. Bioresour Technol **131:**420–428.
28. **Srere PA, Brazil H, Gonen L.** 1963. The citrate condensing enzyme of pigeon breast muscle and moth flight muscle. Acta Chem Scand **17:**129–134.
29. **Gardner JG, Grundy FJ, Henkin TM, Escalante-Semerena JC.** 2006. Control of acetyl-coenzyme A synthetase (AcsA) activity by acetylation/deacetylation without NAD(+) involvement in *Bacillus subtilis*. J Bacteriol **188:**5460–5468. http://dx.doi.org/10.1128/JB.00215-06.
30. **Szurmak B, Wyslouch-Cieszynska A, Wszelaka-Rylik M, Bal W, Dobrzanska M.** 2008. A diadenosine 5′,5″-P1P4 tetraphosphate (Ap4A) hydrolase from Arabidopsis thaliana that is activated preferentially by Mn^{2+} ions. Acta Biochim Pol **55:**151–160.
31. **Koley D, Bard AJ.** 2010. Triton X-100 concentration effects on membrane permeability of a single HeLa cell by scanning electrochemical microscopy (SECM). Proc Natl Acad Sci U S A **107:**16783–16787. http://dx.doi.org/10.1073/pnas.1011614107.
32. **Al-Dabbagh B, Mengin-Lecreulx D, Bouhss A.** 2008. Purification and characterization of the bacterial UDP-GlcNAc:undecaprenyl-phosphate GlcNAc-1-phosphate transferase WecA. J Bacteriol **190:**7141–7146. http://dx.doi.org/10.1128/JB.00676-08.
33. **Thoden JB, Holden HM.** 2007. The molecular architecture of glucose-1-phosphate uridylyltransferase. Protein Sci **16:**432–440. http://dx.doi.org/10.1110/ps.062626007.
34. **Oh E, Becker AH, Sandikci A, Huber D, Chaba R, Gloge F, Nichols RJ, Typas A, Gross CA, Kramer G, Weissman JS, Bukau B.** 2011. Selective ribosome profiling reveals the cotranslational chaperone action of trigger factor *in vivo*. Cell **147:**1295–1308. http://dx.doi.org/10.1016/j.cell.2011.10.044.
35. **Doerrler WT, Sikdar R, Kumar S, Boughner LA.** 2013. New functions for the ancient DedA membrane protein family. J Bacteriol **195:**3–11. http://dx.doi.org/10.1128/JB.01006-12.
36. **Kawai F, Kimura T, Fukaya M, Tani Y, Ogata K, Ueno T, Fukami H.** 1978. Bacterial oxidation of polyethylene glycol. Appl Environ Microbiol **35:**679–684.
37. **Kawai F.** 2002. Microbial degradation of polyethers. Appl Microbiol Biotechnol **58:**30–38. http://dx.doi.org/10.1007/s00253-001-0850-2.
38. **Tasaki Y, Yoshikawa H, Tamura H.** 2006. Isolation and characterization of an alcohol dehydrogenase gene from the octylphenol polyethoxylate degrader *Pseudomonas putida* S-5. Biosci Biotechnol Biochem **70:**1855–1863. http://dx.doi.org/10.1271/bbb.60009.
39. **Alber BE, Spanheimer R, Ebenau-Jehle C, Fuchs G.** 2006. Study of an alternate glyoxylate cycle for acetate assimilation by *Rhodobacter sphaeroides*. Mol Microbiol **61:**297–309. http://dx.doi.org/10.1111/j.1365-2958.2006.05238.x.
40. **Kornberg HL, Krebs HA.** 1957. Synthesis of cell constituents from C_2-units by a modified tricarboxylic acid cycle. Nature **179:**988–991. http://dx.doi.org/10.1038/179988a0.